

1 Glycolytic reprogramming underlies immune cell activation by polyethylene wear 2 particles

3
4 Chima V. Maduka^{1,2,3}, Oluwatosin M. Habeeb^{2,3}, Maxwell M. Kuhnert^{2,3}, Maxwell
5 Hakun^{2,3}, Stuart B. Goodman^{4,5}, Christopher H. Contag^{2,3,6*}

6 ¹ Comparative Medicine & Integrative Biology, Michigan State University, East Lansing, MI 48824, USA

7 ² Department of Biomedical Engineering, Michigan State University, East Lansing, MI 48824, USA

8 ³ Institute for Quantitative Health Science & Engineering, Michigan State University, East Lansing, MI
9 48824, USA

10 ⁴ Department of Orthopedic Surgery, Stanford University, CA 94063, USA.

11 ⁵ Department of Bioengineering, Stanford University, CA 94305, USA.

12 ⁶ Department of Microbiology & Molecular Genetics, Michigan State University, East Lansing, MI 48864,
13 USA.

14 *Christopher H. Contag, contagch@msu.edu

15 **Abstract**

16 Primary total joint arthroplasties (TJAs) are widely and successfully applied reconstructive
17 procedures to treat end-stage arthritis. Nearly 50% of TJAs are now performed in young
18 patients, posing a new challenge: performing TJAs which last a lifetime. The urgency is
19 justified because subsequent TJAs are costlier and fraught with higher complication rates,
20 not to mention the toll taken on patients and their families. Polyethylene particles,
21 generated by wear at joint articulations, drive aseptic loosening by inciting insidious
22 inflammation associated with surrounding bone loss. Down modulating polyethylene
23 particle-induced inflammation enhances integration of implants to bone
24 (osseointegration), preventing loosening. A promising immunomodulation strategy could
25 leverage immune cell metabolism, however, the role of immunometabolism in
26 polyethylene particle-induced inflammation is unknown. Our findings reveal that immune
27 cells exposed to sterile or contaminated polyethylene particles show fundamentally
28 altered metabolism, resulting in glycolytic reprogramming. Inhibiting glycolysis controlled
29 inflammation, inducing a pro-regenerative phenotype that could enhance
30 osseointegration.

31
32 **Keywords:** Polyethylene wear particles, glycolytic reprogramming, total joint
33 arthroplasty, immune cells

34 **Introduction**

35 End-stage arthritis can be successfully treated by primary total joint arthroplasties
36 (TJAs)¹. With nearly 50% of TJAs performed in patients younger than 65 years², the vision
37 of TJAs is now to reconstruct joints which will last a lifetime, despite patients' daily
38 activities³. This is especially crucial because revision TJAs are costlier and fraught with
39 higher complication rates, technical difficulties, and poorer surgical outcomes than
40 primary TJAs⁴. Such revision TJAs commonly arise from aseptic loosening, frequently
41 incited by polyethylene wear particles generated by relative motion at joint articulations⁵.
42 Aseptic loosening may occur with or without adsorbed contaminants, such as bacterial
43 and/or

47 lipopolysaccharides (LPS). Wear particles induce prolonged, low-grade inflammation with
48 macrophages and fibroblasts as key immune cellular players⁶. This pathology is often
49 radiographically detected only when surrounding bone loss (periprosthetic osteolysis)
50 occurs³. By then, compromised implant stability results in loosening and implant failure,
51 necessitating revision surgeries.

52 To minimize generation of wear particles, ultrahigh molecular weight polyethylene
53 liners at the bearing surfaces of reconstructed joints are currently being replaced by highly
54 crosslinked polyethylene. Crosslinked polyethylene has significantly reduced the amount
55 of generated wear particles and accompanied chronic inflammation with periprosthetic
56 osteolysis⁷. However, crosslinking does not completely block the generation of wear
57 particles from bearing surfaces of implants and subsequent inflammation⁸. Up to 9% of
58 patients with crosslinked polyethylene liners present with chronic inflammation-induced
59 periprosthetic osteolysis 15 years later⁹. Moreover, crosslinking has little effect on
60 particles from third body wear, backside wear and impingement¹⁰; and there are currently
61 no agents that specifically treat polyethylene particle-induced inflammatory osteolysis¹¹.
62 Consequently, there is an unmet clinical need to develop methods that will mitigate
63 aseptic loosening from polyethylene particle-induced chronic inflammation to improve
64 implant longevity. Furthermore, as particles generated from ultrahigh molecular weight or
65 highly crosslinked polyethylene similarly result in inflammation^{8,11}, either of them
66 effectively models particle-induced inflammation.

67

68

69

70 Metabolic reprogramming refers to changes in glycolytic flux and oxidative
71 phosphorylation (OXPHOS), traditional bioenergetic pathways, that are inextricably linked
72 to macrophage activation toward proinflammatory^{12,13} or pro-regenerative
73 phenotypes^{14,15}. Advances in understanding macrophage-mesenchymal stem cell
74 crosstalk¹⁶ has revealed that down modulating inflammation induced by polyethylene
75 particles can prevent implant loosening by enhancing osseointegration through increased
76 pro-regenerative macrophage activity. For example, using mesenchymal stem cells
77 (MSCs)¹⁷ and engineered IL-4 expressing MSCs¹⁸; targeting inflammatory pathways
78 using decoy molecules for NF- κ B¹⁹, TNF- α ²⁰ and MCP-1²¹; and using antioxidants like
79 vitamin E¹¹ have shown promise for enhanced osseointegration by reducing
80 inflammation. However, the metabolic underpinnings underlying macrophage activation
81 by polyethylene particles are largely undefined. A detailed understanding of metabolic
82 programs could be leveraged for immunomodulation toward extending the longevity of
83 implants. Here, we show that both macrophages and fibroblasts exposed to sterile or
84 LPS-contaminated polyethylene particles undergo metabolic reprogramming and
85 differential changes in bioenergetics. Glycolytic reprogramming underlies increased
86 levels of proinflammatory cytokines, including MCP-1, IL-6, IL-1 β and TNF- α . Specific
87 inhibition of different glycolytic steps not only modulated these proinflammatory cytokines
88 but stimulated pro-regenerative cytokines, including IL-4 and IL-10, without affecting cell
89 viability. Concomitant elevation of both glycolytic flux and oxidative phosphorylation by
90 polyethylene particles and inhibitory effects on inflammatory cytokines in addition to IL-

91 $1\beta^{13}$ suggest a unique metabolic program that could be targeted for pro-regenerative
92 clinical outcomes following TJAs.

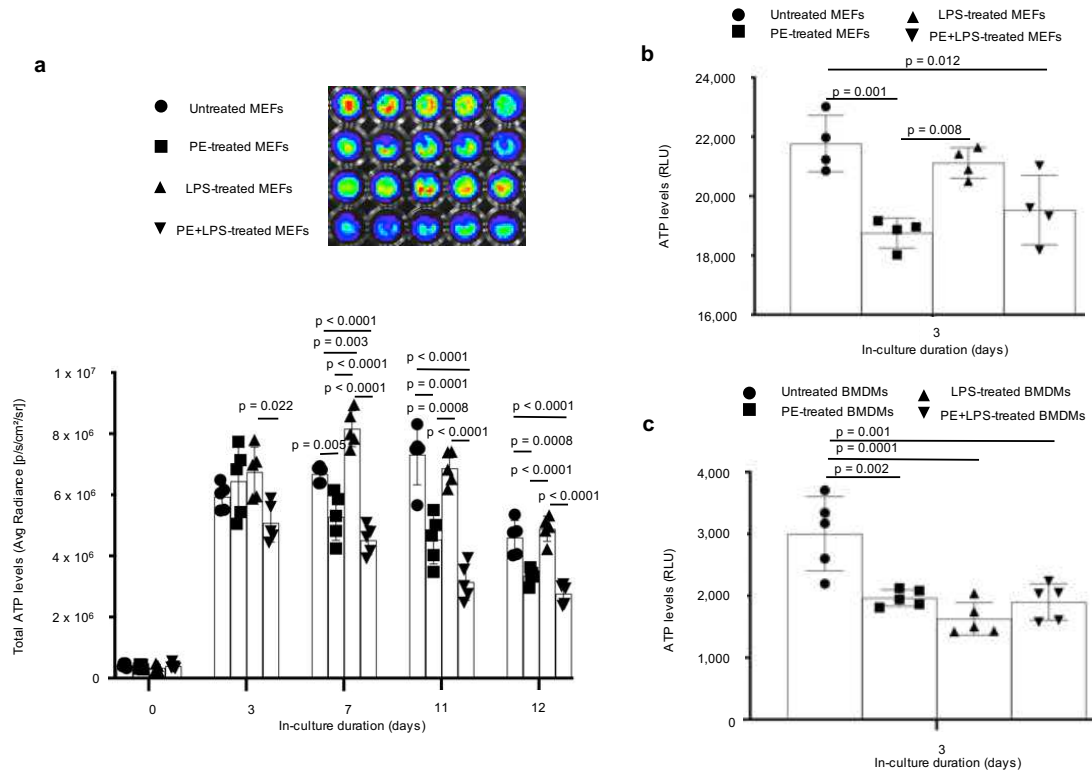


Figure 1 | Ultrahigh molecular weight polyethylene (PE) particles, alone or in combination with endotoxin (LPS), alter bioenergetic (ATP) levels. a, Over time, PE particles lower bioenergetics in blasticidin-eGFP-luciferase (BGL)-transfected mouse embryonic fibroblasts (MEFs) compared to untreated cells; combining PE particles and LPS lowers ATP levels compared to PE particles or LPS alone (representative bioluminescent wells shown). b, In lysed wild-type MEFs, bioenergetics is lowered after exposure to PE particles. c, In primary bone marrow-derived macrophages (BMDMs), PE particles and LPS, alone or in combination, decrease bioenergetics. Mean (SD), n = 5 (Fig. 1a, 1c), n = 4 (Fig. 1b), one-way ANOVA followed by Tukey's post-hoc test.

93

94

Results

95

Bioenergetics is differentially altered in immune cells exposed to polyethylene particles

96

97

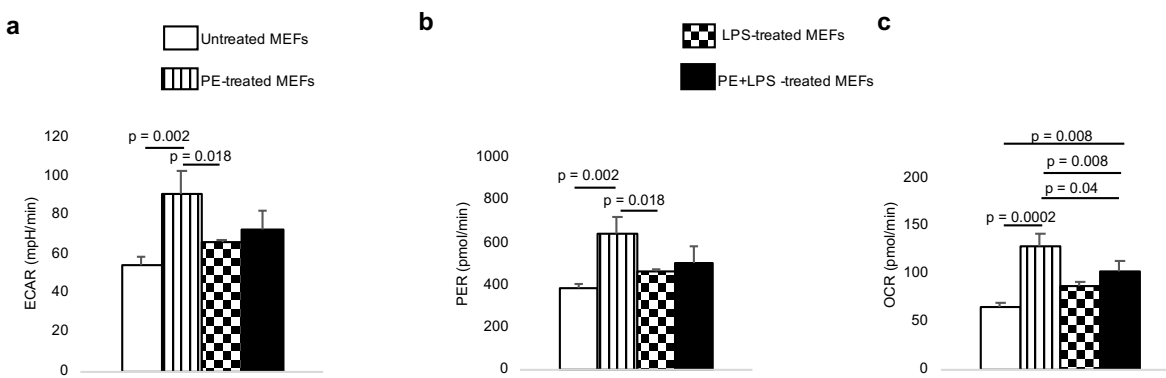
We had previously optimized an in-vitro, live-cell, bioenergetic workflow where ATP is rate-limiting to measure spatiotemporal bioenergetic alterations in cells exposed to biomaterials²². This involved transfecting mouse embryonic fibroblasts (MEFs) with a Sleeping Beauty transposon plasmid (pLuBIG) having a bidirectional promoter driving an improved firefly luciferase gene (fLuc) and a fusion gene encoding a Blasticidin-resistance marker (BsdR) linked to eGFP (BGL)²³. Both highly crosslinked⁸ and ultrahigh molecular weight²¹ polyethylene particles similarly incite inflammation and are clinically used. Ultrahigh molecular weight polyethylene particles whose doses and sizes have been previously characterized were examined herein after polyethylene particles were determined to be endotoxin-free^{17-19,21}. Since adsorbed bacterial lipopolysaccharide (LPS; a.k.a. endotoxin) could play a role in aseptic loosening²⁴, we compared key results to cells exposed to polyethylene particles and LPS.

109 Whereas only polyethylene particles consistently lowered bioenergetic (ATP)
110 levels in live BGL cells, overall, LPS alone did not affect ATP levels when compared to
111 untreated fibroblasts over time (Fig. 1a). In comparison to polyethylene particles or LPS
112 alone, combining polyethylene particles and LPS further decreased ATP levels after
113 prolonged exposure (Fig. 1a). D-luciferin used in live-cell assays could be limited by its
114 ability to permeate cell membranes²⁵; accordingly, bioenergetic measurement in lysed
115 fibroblasts was more sensitive, corroborating decreases in ATP levels after exposure to
116 only polyethylene particles (by 1.2-fold) or a combination of polyethylene particles and
117 LPS (by 1.1-fold) relative to untreated cells at day 3 (Fig. 1b). Primary bone marrow-
118 derived macrophages revealed a 1.5-, 1.8-, and 1.6-fold decrease in ATP levels relative
119 to untreated cells following exposure to only polyethylene particles, only LPS, and
120 polyethylene particles with LPS, respectively (Fig. 1c).

121

122 **Exposure to polyethylene particles alters functional metabolism in immune cells**

123 To explore what bioenergetic pathways were responsible for alterations in ATP
124 levels, we used the Seahorse assay to probe extracellular acidification rate (ECAR),
125 lactate-linked proton efflux rate (PER) and oxygen consumption rate (OCR). ECAR, PER
126 and OCR are indices of glycolytic flux, monocarboxylate transporter (MCT) function^{26,27}
127 and mitochondrial oxidative phosphorylation, respectively, and are used to assess
128 metabolic reprogramming^{12,13}. Following exposure to LPS alone, fibroblasts did not reveal
129 changes in ECAR, PER or OCR compared to untreated cells (Fig. 2a-c). In contrast,
130 exposure to polyethylene particles resulted in a 1.7-, 1.7-, and 2-fold increase in ECAR,
131 PER and OCR, respectively, relative to untreated fibroblasts (Fig. 2a-c). Similarly, a
132 combination of polyethylene particles and LPS increased OCR by 1.6-fold in comparison
133 to untreated fibroblasts (Fig. 2c).



134
135 **Figure 2 | Mouse embryonic fibroblasts (MEFs) exposed to ultrahigh molecular weight polyethylene (PE) particles alone show increased**
136 **functional metabolic indices. a-c, In comparison to untreated cells, PE particle-treated MEFs have higher extracellular acidification rate (ECAR;**
137 **a), proton efflux rate (PER; b) and oxygen consumption rate (OCR; c). Mean (SD), n = 3, one-way ANOVA followed by Tukey's post-hoc test.**

134
135 Exposure to only polyethylene particles increased ECAR, PER and OCR by 13.1-
136 , 13.1- and 3.1-fold, respectively, in primary macrophages compared to untreated cells
137 (Fig. 3a, c, e). Macrophages exposed to polyethylene particles and LPS increased ECAR,

138 PER and OCR by 23-, 23.1- and 2.8-fold, respectively, compared to untreated cells (Fig.
 139 3b, d, f).

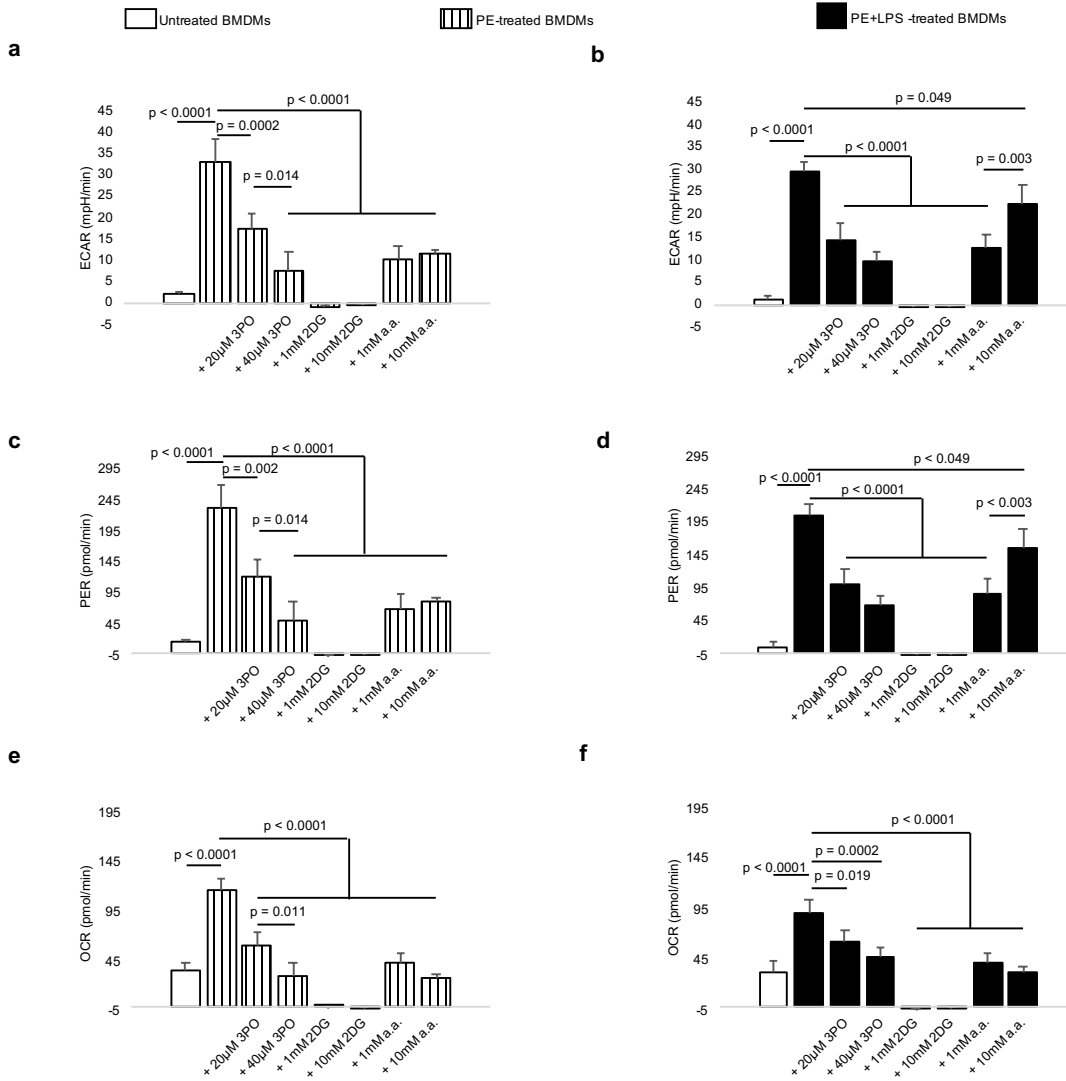


Figure 3 | Primary bone marrow-derived macrophages (BMDMs) exposed to ultrahigh molecular weight polyethylene (PE) particles or both PE particles and endotoxin (LPS) reveal greater extracellular acidification rate (ECAR), proton efflux rate (PER) and oxygen consumption rate (OCR) than untreated cells; this increment is reduced upon addition of various glycolytic inhibitors. a-f, ECAR (a-b), PER (c-d) and OCR (e-f) are increased in BMDMs treated with PE particles, alone or in combination with LPS; elevated levels are decreased upon addition of 3-(3-Pyridinyl)-1-(4-pyridinyl)-2-propen-1-one (3PO), 2-deoxyglucose (2DG) or aminoxyacetic acid (a.a.). Mean (SD), n = 3, one-way ANOVA followed by Tukey's post-hoc test.

140
 141 To reduce abnormal increments in ECAR, PER and OCR, we targeted different
 142 stages of glycolysis using 3-(3-pyridinyl)-1-(4-pyridinyl)-2-propen-1-one (3PO), 2-
 143 deoxyglucose (2DG) and aminoxyacetic acid (a.a.). 3PO inhibits 6-phosphofructo-2-
 144 kinase which is the rate limiting glycolytic enzyme²⁸; 2DG inhibits hexokinase, the first
 145 enzyme in glycolysis¹³; and a.a. prevents the mitochondrion from utilizing glycolytic
 146 pyruvate²⁹. In a dose-dependent manner, 3PO, 2DG and a.a. decreased ECAR, PER and
 147 OCR among macrophages exposed to only polyethylene particles or a combination of

148 polyethylene particles and LPS (Fig. 3a-f), suggesting efficient cellular uptake and
 149 pharmacologic effects of these small molecule inhibitors.

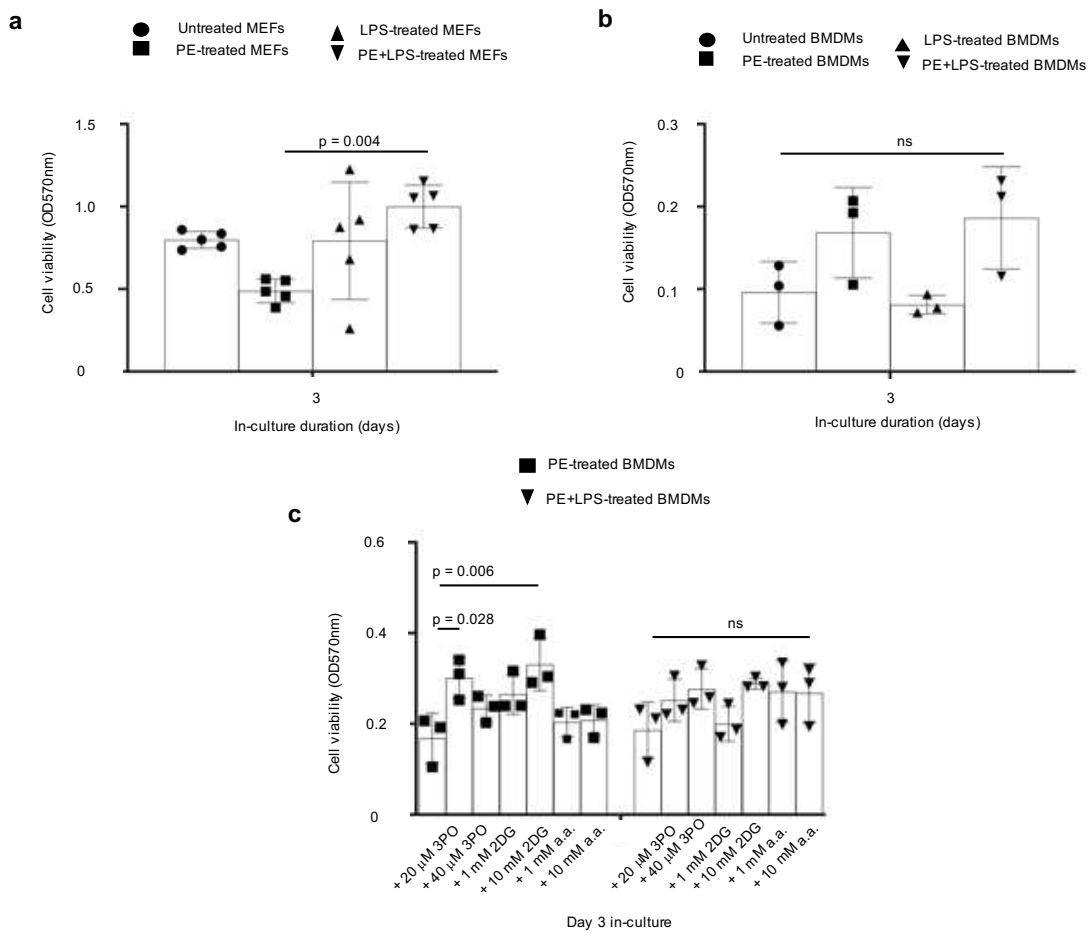


Figure 4 | Compared to untreated cells, treatment with ultrahigh molecular weight polyethylene (PE) particles, endotoxin (LPS) or a combination of PE particles and LPS does not change cell numbers; addition of glycolytic inhibitors does not decrease cell numbers. a-b. In mouse embryonic fibroblasts (MEFs; a) or primary bone marrow-derived macrophages (BMDMs; b), exposure to PE particles, LPS or PE particles and LPS does not change cell numbers relative to untreated controls. c. Addition of various doses of 3-(3-Pyridinyl)-1-(4-pyridinyl)-2-propen-1-one (3PO), 2-deoxyglucose (2DG) or aminooxyacetic acid (a.a.) to PE particle-treated or PE particle- and LPS-treated BMDMs does not decrease cell numbers. Mean (SD), n = 5 (Fig. 4a), n = 3 (Fig. 4b, c), one-way ANOVA followed by Tukey's post-hoc test.

150
 151 Compared to untreated cells, there was no difference in cell numbers following
 152 exposure to polyethylene particles, LPS or polyethylene particles with LPS among
 153 fibroblasts (Fig. 4a) or macrophages (Fig. 4b). Additionally, exposure of macrophages to
 154 pharmacologic inhibitors, including 3PO, 2DG and a.a. did not lower cell viability (Fig. 4c).
 155 Importantly, in fibroblasts exposed to polyethylene particles alone or polyethylene
 156 particles and LPS, addition of 3PO, 2DG or a.a. further lowered bioenergetics in a dose-
 157 dependent manner (Fig. 5).
 158

159 Immunometabolism underlies macrophage polarization by polyethylene particles

160 To evaluate how metabolism affects immune cellular function, we assayed levels
 161 of cytokine and chemokine expression using a magnetic bead-based technique³⁰. We
 162 observed that proinflammatory proteins, including MCP-1 (Fig. 6a), IL-6 (Fig. 6b), IL-1 β

163 (Fig. 6c) and TNF- α (Fig. 6d) were increased by 4.1-, 97.3-, 41.8- and 7-fold, respectively,
164 after exposure to polyethylene particles in comparison to untreated macrophages.

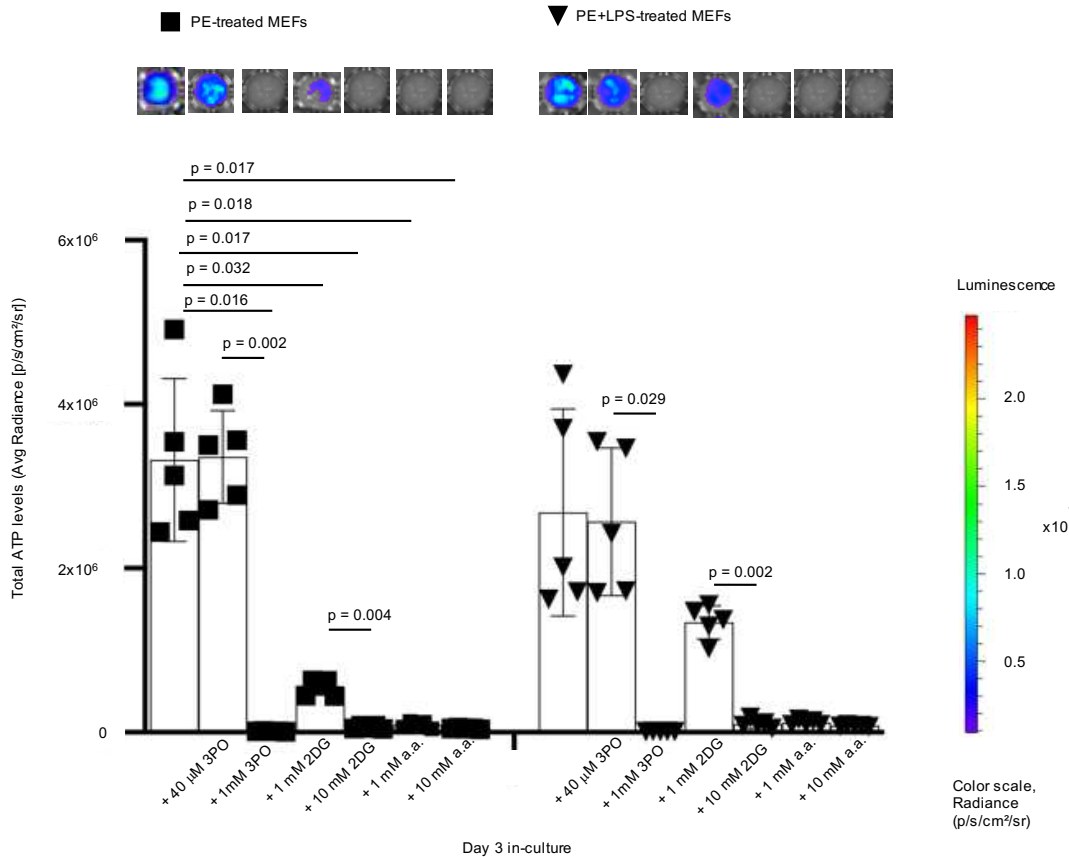


Figure 5 | Glycolytic inhibitors decrease bioenergetic levels in treated mouse embryonic fibroblasts (MEFs). Following treatment of blasticidin-GFP-Luciferase (BGL)-transfected MEFs with ultrahigh molecular weight polyethylene (PE) particles alone or in combination with endotoxin (LPS), addition of 3-(3-pyridinyl)-1-(4-pyridinyl)-2-propen-1-one (3PO), 2-deoxyglucose (2DG) and aminoxyacetic acid (a.a.; representative wells are shown) tend to decrease bioenergetics in a dose-dependent manner. Not significant (ns), mean (SD), Brown-Forsythe and Welch ANOVA followed by Dunnett's T3 multiple comparisons test, n = 5.

165
166 Addition of 3PO or 2DG consistently decreased proinflammatory cytokine or
167 chemokine levels (Fig. 6a-d) relative to macrophages exposed to only polyethylene
168 particles; however, addition of a.a. selectively decreased MCP-1 expression (Fig. 6a).
169 Exposure of macrophages to polyethylene particles decreased IL-4 levels by 7.4-fold
170 compared to untreated cells; addition of 3PO, 2DG or a.a. increased IL-4 levels by 2.9-,
171 4.3-, and 1.5- fold, respectively, relative to polyethylene particles alone; however, only the
172 increase by 2DG was statistically significant (Fig. 6e). Levels of IL-13 and IFN- λ were
173 unchanged (data not shown). Consistent with macrophage polarization being a
174 continuum^{31,32}, polyethylene particles increased IL-10 expression in comparison to
175 untreated macrophages (Fig. 6f). Whereas addition of 3PO or 2DG did not increase IL-
176 10 levels, a.a. increased IL-10 expression by 3.2-fold relative to macrophages exposed
177 to only polyethylene particles (Fig. 6f).

178

179

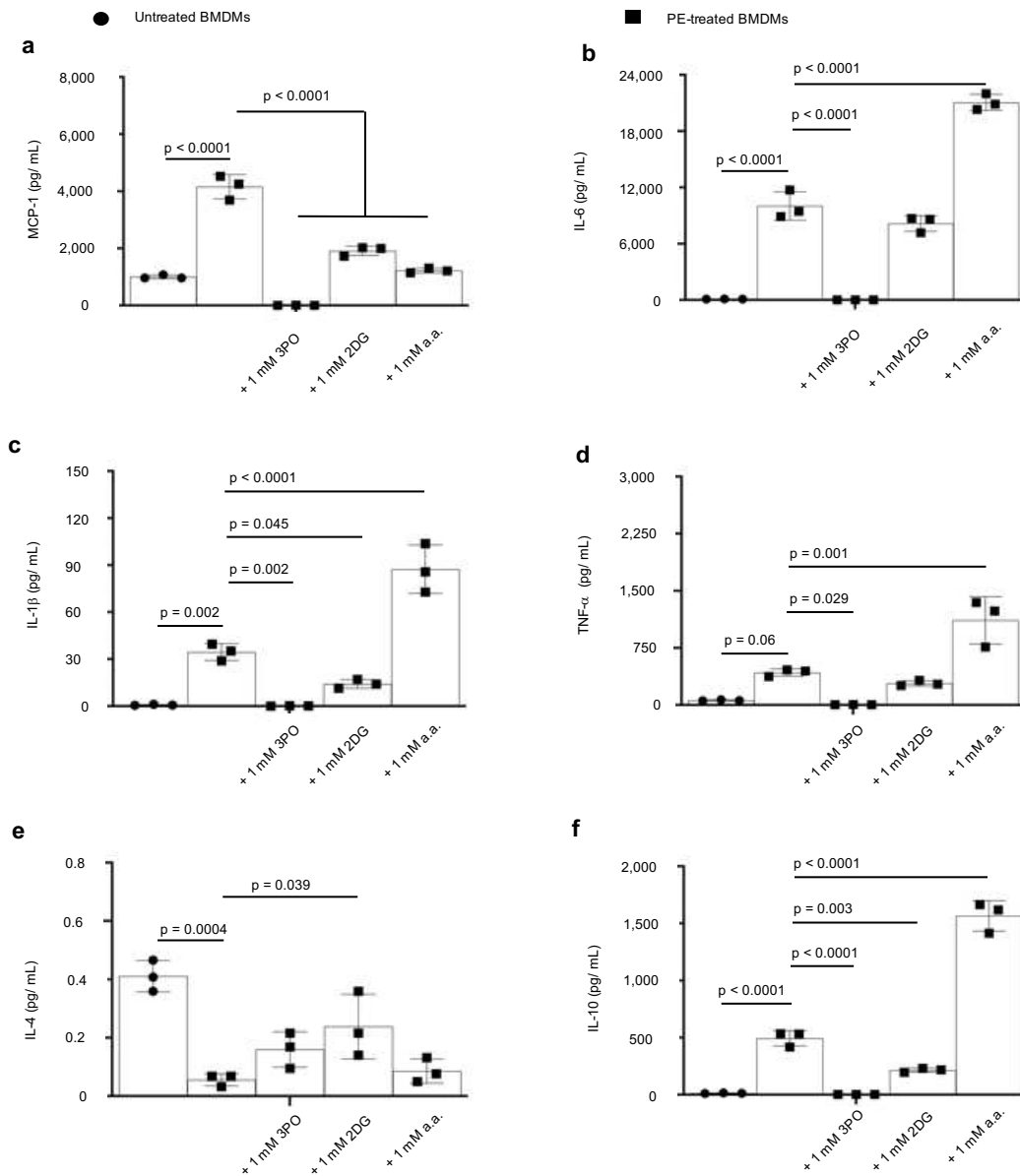


Figure 6 | Elevated proinflammatory cytokine (protein) levels are decreased following addition of glycolytic inhibitors to primary bone marrow-derived macrophages (BMDMs). **a-d**, In BMDMs, exposure to ultrahigh molecular weight polyethylene (PE) particles increase proinflammatory cytokines, including MCP-1 (**a**), IL-6 (**b**), IL-1 β (**c**) and TNF- α (**d**) in comparison to untreated BMDMs. Addition of 3-(3-Pyridinyl)-1-(4-pyridinyl)-2-propen-1-one (3PO) or 2-deoxyglucose (2DG) decreases proinflammatory cytokines; aminoxyacetic acid (a.a.) selectively decreases MCP-1 levels. **e**, Exposure of BMDMs to PE particles decreases IL-4 levels in comparison to untreated cells; IL-4 levels tend to increase following addition of glycolytic inhibitors. **f**, Compared to BMDMs exposed to only PE particles, exposure to PE particles and a.a. increase IL-10 levels. Mean (SD), n = 3, one-way ANOVA followed by Tukey's post-hoc test; assay was performed after 3 days in-culture.

180 Discussion

181 When macrophages are exposed to bacterial lipopolysaccharide (LPS), their
 182 bioenergetic (ATP) levels are decreased as part of cell activation and inflammation³³. This
 183 results from reprogrammed metabolism that shifts bioenergetic dependence from
 184 mitochondrial oxidative phosphorylation (OXPHOS) to glycolysis, with crucial
 185 consequences on proinflammatory^{12,13} and anti-inflammatory^{14,15} events. While
 186 immunometabolism in response to LPS has been well characterized for such clinical
 187 applications as bacterial sepsis, the role of immunometabolism in sterile inflammation
 188 induced by clinically relevant implant materials is unknown.

189 Macrophages are the dominant immune cell type implicated in the chronic
190 inflammatory response to ultrahigh molecular weight polyethylene (PE) particles², likely
191 acting through Toll-like receptors (TLRs)^{34,35}. Following exposure to PE particles of
192 particular sizes and over a threshold, transcriptional signaling occurs through NF- κ B³⁶,
193 MyD88³⁷ and chemerin/ChemR23³⁸. Consequently, there is increased production of
194 proinflammatory cytokines that accompany resulting pathologies, including periprosthetic
195 osteolysis. Likewise, fibroblasts play a synergistic role with macrophages. Fibroblasts
196 exposed to PE particles^{39,40} express MCP-1, RANKL, IL-1 β , IL-6, MMP1 and MMP2
197 which activate osteoclasts, accentuate inflammation and degrade surrounding bone
198 extracellular matrix.

199 Adsorbed LPS could be a contaminant on sterilized implants and has been
200 documented in a subset of patients diagnosed with aseptic loosening of implants from
201 chronic inflammation²⁴, and could exacerbate PE particle-induced inflammation⁴¹.
202 Therefore, PE and LPS-contaminated PE (cPE) particles were examined and compared
203 to LPS. Our findings reveal that bioenergetic imbalances differentially occur in
204 macrophages and fibroblasts exposed to PE particles, LPS or cPE particles. For example,
205 although LPS did not affect ATP levels in fibroblasts, PE particles lowered cellular
206 bioenergetics. Furthermore, fibroblasts exposed to PE particles but not LPS were
207 metabolically reprogrammed, revealing increases in glycolysis, OXPHOS and
208 monocarboxylate transporter (MCT) function. On the other hand, decreased ATP levels
209 were observed in primary bone marrow-derived macrophages exposed to PE particles,
210 LPS or cPE particles consistent with reliance on glycolysis. Immune cells depend on
211 glycolysis during inflammatory activation as glycolysis produces ATP quicker than
212 OXPHOS, albeit OXPHOS results in overall higher ATP levels. Additionally, this switch to
213 glycolysis is crucial for IL-1 β production by stabilizing HIF-1 α in macrophages¹³ and
214 fibroblast activation in fibrosis⁴². Surprisingly, in addition to elevated glycolysis, OXPHOS
215 was increased in macrophages exposed to PE or cPE particles, independent of changing
216 cell numbers. Concomitant elevation in both glycolysis and OXPHOS suggests a unique
217 metabolic reprogram induced by PE particles relative to LPS; LPS increases glycolysis
218 while reducing OXPHOS¹². Accompanied decrease in ATP levels suggests that increased
219 OXPHOS is directed at functions other than cellular energy supply. In a septic model,
220 LPS was shown to repurpose mitochondrial function toward superoxide formation in
221 macrophages¹². At earlier time points than used in this study, LPS decreased OXPHOS¹²,
222 likely reflecting as yet uncharacterized temporal changes in metabolic reprogramming.
223 Notably, glycolytic flux and MCT function but not OXPHOS were higher in macrophages
224 exposed to cPE than PE particles, relative to respective controls. This may likely be from
225 synergistic signaling with cPE particles, as PE particles and LPS are known to activate
226 TLR2 and TLR4 receptors, respectively^{34,35}.

227 Elevated glycolytic flux in macrophages exposed to PE or cPE particles could be
228 lowered by specific pharmacologic inhibition of different glycolytic steps using 3-(3-
229 pyridinyl)-1-(4-pyridinyl)-2-propen-1-one (3PO)²⁸, 2-deoxyglucose (2DG)¹³ and
230 aminoxyacetic acid (a.a.)²⁹. Lactate from glycolysis is converted to pyruvate which feeds
231 mitochondrial OXPHOS, and proton-linked lactate is bidirectionally shuttled through
232 MCT^{26,27}. Consequently, pharmacologic inhibition of glycolysis lowered aberrantly

233 elevated OXPHOS and MCT function. Pharmacologic inhibition did not result in reduced
234 cell viability, excluding potential toxicity. Using fibroblasts expressing luciferase, we
235 observed that glycolytic inhibition further reduced ATP levels following exposure to PE
236 particles, corroborating cellular bioenergetic dependence on glycolysis.

237 Contrasting non-degradable PE, polylactide (PLA) is a biodegradable biomaterial.
238 Degradation products of PLA, oligomers and monomers of lactic acid, increase ATP
239 levels only after prolonged exposure to immune cells, modeling in-vivo conditions²².
240 Increased ATP levels are the result of elevated flux in both glycolysis and mitochondrial
241 respiration, in-vitro. Corroborating in-vitro observations, radiolabeled glucose uptake was
242 elevated in a subcutaneous model and shown to drive inflammation to sterile PLA;
243 targeting glycolysis in-vivo decreased inflammatory markers, including CD86, by reducing
244 radiolabeled glucose uptake. Similarly, in patients who have undergone total joint
245 arthroplasties, chronic inflammation by PE particles is often diagnosed by increased
246 glycolytic flux. Glycolytic flux is measured using fluorodeoxyglucose in positron emission
247 tomography (PET) combined with computed tomography (CT) or magnetic resonance
248 imaging (MRI)⁴³⁻⁴⁶. Our findings suggests that PET imaging is enabled by glycolytic
249 reprogramming of immune cells in inflamed joints, following exposure to PE or cPE
250 particles.

251 Macrophages exposed to PE particles became polarized to a proinflammatory
252 phenotype as measured by elevated protein expression of MCP-1, IL-6, IL-1 β and TNF- α . Additionally, IL-10 was increased, consistent with macrophage polarization being a
253 spectrum³¹. Both IL-1 β and TNF- α induce RANKL expression which drives osteoclast
254 maturation and differentiation, together with M-CSF⁶. Osteolysis, associated with PE
255 particle-induced chronic inflammation, is the result of net bone loss from osteoclast-
256 mediated bone resorption exceeding osteoblast-mediated bone formation. Similarly, IL-
257 6⁴⁷ and MCP-1⁴⁸ are associated with increased osteolysis and cartilage destruction.
258 Interestingly, 2DG and 3PO decreased aberrantly elevated proinflammatory cytokines. In
259 particular, 2DG allowed for some level of proinflammatory cytokine expression. This is
260 clinically important because a suitable level of inflammation is required for tissue repair
261 and osseointegration⁴⁹; compromised osseointegration is a leading cause of implant
262 failure⁴. Remarkably, whereas 2DG decreased MCP-1, IL-6, IL-1 β and TNF- α protein
263 levels which were elevated by PE particles, 2DG is known to selectively decrease IL-1 β
264 protein levels from LPS¹³, suggesting unique differences. In contrast to 2DG and 3PO,
265 a.a. selectively decreased MCP-1 but not IL-6, IL-1 β and TNF- α ; and increased IL-10
266 levels. Central to macrophage-stem cell crosstalk, IL-10 signaling is critical for tissue
267 regeneration⁵⁰. Glycolytic inhibition using 2DG increased IL-4 levels which were reduced
268 by PE particles. Increment of IL-4 levels suggest a pro-regenerative macrophage
269 phenotype. Acute and chronic inflammation as well as bone loss induced by PE particles
270 is reversed by inducing a pro-regenerative macrophage phenotype using IL-4¹⁸.

272 In conclusion, all clinically relevant biomaterials undergo wear at articulations,
273 resulting in different levels of chronic inflammation and undermining the longevity of
274 biomaterials used in arthroplasties. By characterizing immune cell metabolism as being
275 pivotal in the inflammatory pathology induced by polyethylene particles, we reveal a
276 unique vulnerability which could be harnessed for the dual purposes of controlling

277 inflammation and stimulating pro-regenerative immune cell phenotypes. Targeting
278 immunometabolism can be extended to other implant materials^{51,52}, improving
279 osseointegration and long-term clinical outcomes for patients undergoing various
280 arthroplasties.

281

282 **Methods**

283 **Materials.** Ultrahigh molecular weight polyethylene particles were sourced, characterized
284 and determined to be endotoxin-free as previously described¹⁸. Concentrations of 100ng/
285 mL of lipopolysaccharide (LPS) from *Escherichia coli* O111:B4 (MilliporeSigma) and 1.25
286 mg/ mL of ultrahigh molecular weight polyethylene particles were used. Furthermore, 3-
287 (3-pyridinyl)-1-(4-pyridinyl)-2-propen-1-one (MilliporeSigma), 2-deoxyglucose
288 (MilliporeSigma) and aminoxyacetic acid (Sigma-Aldrich) were used for glycolytic
289 inhibition.

290

291 **Bioenergetic measurement.** Bioluminescence was measured using the IVIS Spectrum
292 in vivo imaging system (PerkinElmer) after adding 150 µg/mL of D-luciferin (PerkinElmer).
293 Living Image (Version 4.5.2, PerkinElmer) was used for acquiring bioluminescence on the
294 IVIS Spectrum. Standard ATP/ADP kits (Sigma-Aldrich) containing D-luciferin, luciferase
295 and cell lysis buffer were used to according to manufacturer's instructions. Luminescence
296 at integration time of 1,000 ms was obtained using the SpectraMax M3
297 Spectrophotometer (Molecular Devices) using SoftMax Pro (Version 7.0.2, Molecular
298 Devices).

299

300 **Cells.** Mouse embryonic fibroblast (MEFs) cell line (NIH 3T3 cell line; ATCC) and primary
301 bone-marrow derived macrophages (BMDMs) derived from C57BL/6J mice (Jackson
302 Laboratories) of 3-4 months^{12,53} were used. NIH 3T3 cells were stably transfected with a
303 Sleeping Beauty transposon plasmid (pLuBIG) having a bidirectional promoter driving an
304 improved firefly luciferase gene (fLuc) and a fusion gene encoding a Blasticidin-resistance
305 marker (BsdR) linked to eGFP (BGL)²³. This enabled us to monitor bioenergetic changes
306 in live cells²². For temporal (IVIS) experiments lasting 12 days, 5,000 BGL cells were
307 initially seeded in each well of a 96-well tissue culture plate in 200 µL of complete medium
308 (see below). For ATP, crystal violet and Seahorse assays, 20,000 wild-type MEFs were
309 seeded. For ATP, crystal violet and cytokine/ chemokine assays, 50,000 BMDMs were
310 seeded; 60,000 BMDMs were seeded for Seahorse experiments. For IVIS experiments
311 with glycolytic inhibitors, 20,000 BGL cells were initially seeded. All time points are
312 indicated on respective graphs. Complete medium comprised of DMEM medium, 10%
313 heat-inactivated Fetal Bovine Serum and 100 U/mL penicillin-streptomycin (all from
314 ThermoFisher Scientific).

315

316 **Cell viability.** Cell viability was assessed using the crystal violet assay⁵⁴. Absorbance
317 (optical density) was acquired at 570 nm using the the SpectraMax M3
318 Spectrophotometer (Molecular Devices) and SoftMax Pro software (Version 7.0.2,
319 Molecular Devices).

320

321 **Functional metabolism.** Basal measurements of oxygen consumption rate (OCR),
322 extracellular acidification rate (ECAR) and lactate-linked proton efflux rate (PER) were
323 obtained in real-time using the Seahorse XFe-96 Extracellular Flux Analyzer (Agilent
324 Technologies)^{12,13,15}. Prior to running the assay, cell culture medium was replaced by the
325 Seahorse XF DMEM medium (pH 7.4) supplemented with 25 mM D-glucose and 4 mM
326 Glutamine. The Seahorse ATP rate assay was run according to manufacturer's instruction
327 and all reagents for the Seahorse assays were sourced from Agilent Technologies. Wave
328 software (Version 2.6.1) was used to export Seahorse data directly as means \pm standard
329 deviation (SD).

330

331 **Chemokine and cytokine measurements.** Cytokine and chemokine levels were
332 measured using a MILLIPLEX MAP mouse magnetic bead multiplex kit (MilliporeSigma)³⁰
333 to assess for IL-6, MCP-1, TNF- α , IL-1 β , IL-4, IL-10, IFN- λ and 1L-13 protein expression
334 in supernatants. Data was acquired using Luminex 200 (Luminex Corporation) by the
335 xPONENT software (Version 3.1, Luminex Corporation). Using the glycolytic inhibitor,
336 3PO, expectedly decreased cytokine values to < 3.2 pg/ mL in some experiments. For
337 statistical analyses, those values were expressed as 3.1 pg/ mL. Values exceeding the
338 dynamic range of the assay, in accordance with manufacturer's instruction, were
339 excluded. Additionally, IL-6 ELISA kits (RayBiotech) for supernatants were used
340 according to manufacturer's instructions.

341

342 **Statistics and reproducibility.** Statistical software (GraphPad Prism) was used to
343 analyse data presented as mean with standard deviation (SD). Significance level was
344 set at $p < 0.05$, and details of statistical tests and sample sizes, which are biological
345 replicates, are provided in figure legends. Exported data (mean, SD) from Wave in
346 Seahorse experiments had the underlying assumption of normality and similar variance,
347 and thus were tested using corresponding parametric tests as indicated in figure
348 legends.

349

350

351 **References**

- 352 1 Ingham, E. & Fisher, J. Biological reactions to wear debris in total joint replacement.
353 *Proceedings of the Institution of Mechanical Engineers, Part H: Journal of Engineering in*
354 *Medicine* **214**, 21-37 (2000).
- 355 2 Cobelli, N., Scharf, B., Crisi, G. M., Hardin, J. & Santambrogio, L. Mediators of the
356 inflammatory response to joint replacement devices. *Nature Reviews Rheumatology* **7**,
357 600-608 (2011).
- 358 3 Sivananthan, S., Goodman, S. & Burke, M. in *Joint Replacement Technology* 373-402
359 (Elsevier, 2021).
- 360 4 Goodman, S. B., Gallo, J., Gibon, E. & Takagi, M. Diagnosis and management of implant
361 debris-associated inflammation. *Expert review of medical devices* **17**, 41-56 (2020).
- 362 5 Bistolfi, A. *et al.* Ultra-high molecular weight polyethylene (UHMWPE) for hip and knee
363 arthroplasty: The present and the future. *Journal of Orthopaedics* **25**, 98-106 (2021).

364 6 Kandahari, A. M. *et al.* A review of UHMWPE wear-induced osteolysis: the role for early
365 detection of the immune response. *Bone research* **4**, 1-13 (2016).

366 7 Tsukamoto, M., Mori, T., Ohnishi, H., Uchida, S. & Sakai, A. Highly cross-linked
367 polyethylene reduces osteolysis incidence and wear-related reoperation rate in
368 cementless total hip arthroplasty compared with conventional polyethylene at a mean
369 12-year follow-up. *The Journal of Arthroplasty* **32**, 3771-3776 (2017).

370 8 Ormsby, R. T. *et al.* Osteocytes respond to particles of clinically-relevant conventional
371 and cross-linked polyethylene and metal alloys by up-regulation of resorptive and
372 inflammatory pathways. *Acta biomaterialia* **87**, 296-306 (2019).

373 9 Hopper Jr, R. H., Ho, H., Sritulanondha, S., Williams, A. C. & Engh Jr, C. A. Otto Aufranc
374 Award: crosslinking reduces THA wear, osteolysis, and revision rates at 15-year followup
375 compared with noncrosslinked polyethylene. *Clinical orthopaedics and related research*
376 **476**, 279 (2018).

377 10 Greenfield, E. M. *et al.* Does endotoxin contribute to aseptic loosening of orthopedic
378 implants? *Journal of Biomedical Materials Research Part B: Applied Biomaterials: An
379 Official Journal of The Society for Biomaterials, The Japanese Society for Biomaterials,
380 and The Australian Society for Biomaterials and the Korean Society for Biomaterials* **72**,
381 179-185 (2005).

382 11 Liu, F., Dong, J., Zhou, D. & Zhang, Q. Identification of key candidate genes related to
383 inflammatory osteolysis associated with vitamin E-Blended UHMWPE debris of
384 orthopedic implants by integrated bioinformatics analysis and experimental
385 confirmation. *Journal of Inflammation Research* **14**, 3537 (2021).

386 12 Mills, E. L. *et al.* Succinate Dehydrogenase Supports Metabolic Repurposing of
387 Mitochondria to Drive Inflammatory Macrophages. *Cell* **167**, 457-470.e413,
388 doi:10.1016/j.cell.2016.08.064 (2016).

389 13 Tannahill, G. *et al.* Succinate is a danger signal that induces IL-1 β via HIF-1 α . *Nature* **496**,
390 238-242, doi:10.1038/nature11986 (2013).

391 14 Mills, E. L. *et al.* Itaconate is an anti-inflammatory metabolite that activates Nrf2 via
392 alkylation of KEAP1. *Nature* **556**, 113 (2018).

393 15 Ip, W. E., Hoshi, N., Shouval, D. S., Snapper, S. & Medzhitov, R. Anti-inflammatory effect
394 of IL-10 mediated by metabolic reprogramming of macrophages. *Science* **356**, 513-519
395 (2017).

396 16 Pajarin, J. *et al.* Mesenchymal stem cell-macrophage crosstalk and bone healing.
397 *Biomaterials* **196**, 80-89 (2019).

398 17 Lin, T. *et al.* Preconditioning of murine mesenchymal stem cells synergistically enhanced
399 immunomodulation and osteogenesis. *Stem cell research & therapy* **8**, 1-9 (2017).

400 18 Pajarin, J. *et al.* Interleukin-4 repairs wear particle induced osteolysis by modulating
401 macrophage polarization and bone turnover. *Journal of Biomedical Materials Research
402 Part A* **109**, 1512-1520 (2021).

403 19 Lin, T.-H. *et al.* NF- κ B decoy oligodeoxynucleotide enhanced osteogenesis in
404 mesenchymal stem cells exposed to polyethylene particle. *Tissue engineering Part A* **21**,
405 875-883 (2015).

406 20 Zhao, Y.-p. *et al.* Programulin suppresses titanium particle induced inflammatory
407 osteolysis by targeting TNF α signaling. *Scientific reports* **6**, 1-13 (2016).

408 21 Gibon, E. *et al.* Selective inhibition of the MCP-1-CCR2 ligand-receptor axis decreases
409 systemic trafficking of macrophages in the presence of UHMWPE particles. *Journal of*
410 *Orthopaedic Research* **30**, 547-553 (2012).

411 22 Maduka, C. V. *et al.* Polylactide Degradation Activates Immune Cells by Metabolic
412 Reprogramming. *bioRxiv* (2022).

413 23 Kanada, M. *et al.* Differential fates of biomolecules delivered to target cells via
414 extracellular vesicles. *Proceedings of the National Academy of Sciences* **112**, E1433-
415 E1442 (2015).

416 24 Bonsignore, L. A., Anderson, J. R., Lee, Z., Goldberg, V. M. & Greenfield, E. M. Adherent
417 lipopolysaccharide inhibits the osseointegration of orthopedic implants by impairing
418 osteoblast differentiation. *Bone* **52**, 93-101 (2013).

419 25 Lee, K. *et al.* Cell uptake and tissue distribution of radioiodine labelled D-luciferin:
420 implications for luciferase based gene imaging. *Nuclear medicine communications* **24**,
421 1003-1009 (2003).

422 26 Tan, Z. *et al.* in *The Journal of biological chemistry* Vol. 290 46-55 (2015).

423 27 Payen, V. L., Mina, E., Van Hee, V. F., Porporato, P. E. & Sonveaux, P. Monocarboxylate
424 transporters in cancer. *Mol Metab* **33**, 48-66, doi:10.1016/j.molmet.2019.07.006 (2020).

425 28 Clem, B. *et al.* Small-molecule inhibition of 6-phosphofructo-2-kinase activity suppresses
426 glycolytic flux and tumor growth. *Molecular cancer therapeutics* **7**, 110-120 (2008).

427 29 Kauppinen, R. A., Sihra, T. S. & Nicholls, D. G. Aminooxyacetic acid inhibits the malate-
428 aspartate shuttle in isolated nerve terminals and prevents the mitochondria from
429 utilizing glycolytic substrates. *Biochim Biophys Acta* **930**, 173-178, doi:10.1016/0167-
430 4889(87)90029-2 (1987).

431 30 Sprague, L. *et al.* Dendritic cells: in vitro culture in two-and three-dimensional collagen
432 systems and expression of collagen receptors in tumors and atherosclerotic
433 microenvironments. *Experimental cell research* **323**, 7-27 (2014).

434 31 Sadtler, K. *et al.* Design, clinical translation and immunological response of biomaterials
435 in regenerative medicine. *Nature Reviews Materials* **1**, 1-17 (2016).

436 32 Mishra, P. K. *et al.* Sterile particle-induced inflammation is mediated by macrophages
437 releasing IL-33 through a Bruton's tyrosine kinase-dependent pathway. *Nature materials*
438 **18**, 289-297 (2019).

439 33 O'Neill, L. A. & Pearce, E. J. in *J Exp Med* Vol. 213 15-23 (2016).

440 34 Maitra, R., Clement, C. C., Crisi, G. M., Cobelli, N. & Santambrogio, L. Immunogenicity of
441 modified alkane polymers is mediated through TLR1/2 activation. *PLoS one* **3**, e2438
442 (2008).

443 35 Tamaki, Y. *et al.* Increased expression of toll-like receptors in aseptic loose
444 periprosthetic tissues and septic synovial membranes around total hip implants. *The*
445 *Journal of rheumatology* **36**, 598-608 (2009).

446 36 Hedges, N. A., Sussman, E. M. & Stegemann, J. P. Aseptic and septic prosthetic joint
447 loosening: Impact of biomaterial wear on immune cell function, inflammation, and
448 infection. *Biomaterials* **278**, 121127 (2021).

449 37 Goodman, S. B., Pajarin, J., Yao, Z. & Lin, T. Inflammation and bone repair: from
450 particle disease to tissue regeneration. *Frontiers in Bioengineering and Biotechnology*,
451 230 (2019).

452 38 Zhao, F., Cang, D., Zhang, J. & Zheng, L. Chemerin/ChemR23 signaling mediates the
453 effects of ultra-high molecular weight polyethylene wear particles on the balance
454 between osteoblast and osteoclast differentiation. *Annals of Translational Medicine* **9**
455 (2021).

456 39 Koreny, T. *et al.* The role of fibroblasts and fibroblast-derived factors in periprosthetic
457 osteolysis. *Arthritis & Rheumatism: Official Journal of the American College of*
458 *Rheumatology* **54**, 3221-3232 (2006).

459 40 Man, K., Jiang, L.-H., Foster, R. & Yang, X. B. Immunological responses to total hip
460 arthroplasty. *Journal of functional biomaterials* **8**, 33 (2017).

461 41 Dapunt, U., Prior, B., Kretzer, J. P., Giese, T. & Zhao, Y. Bacterial Biofilm Components
462 Induce an Enhanced Inflammatory Response Against Metal Wear Particles. *Therapeutics*
463 *and clinical risk management* **16**, 1203 (2020).

464 42 Xie, N. *et al.* Glycolytic reprogramming in myofibroblast differentiation and lung fibrosis.
465 *American journal of respiratory and critical care medicine* **192**, 1462-1474 (2015).

466 43 Kisielinski, K., Cremerius, U., Reinartz, P. & Niethard, F. Fluorodeoxyglucose positron
467 emission tomography detection of inflammatory reactions due to polyethylene wear in
468 total hip arthroplasty. *The Journal of arthroplasty* **18**, 528-532 (2003).

469 44 Reinartz, P. *et al.* Radionuclide imaging of the painful hip arthroplasty: positron-emission
470 tomography versus triple-phase bone scanning. *The Journal of Bone and Joint Surgery.*
471 *British volume* **87**, 465-470 (2005).

472 45 Kuo, J., Foster, C. & Shelton, D. Particle disease on fluoride-18 (NaF) PET/CT imaging.
473 *Journal of Radiology Case Reports* **5**, 24 (2011).

474 46 van der Bruggen, W., Bleeker-Rovers, C. P., Boerman, O. C., Gotthardt, M. & Oyen, W. J.
475 in *Seminars in nuclear medicine*. 3-15 (Elsevier).

476 47 Udagawa, N. *et al.* Interleukin (IL)-6 induction of osteoclast differentiation depends on
477 IL-6 receptors expressed on osteoblastic cells but not on osteoclast progenitors. *The*
478 *Journal of experimental medicine* **182**, 1461-1468 (1995).

479 48 Raghu, H. *et al.* CCL2/CCR2, but not CCL5/CCR5, mediates monocyte recruitment,
480 inflammation and cartilage destruction in osteoarthritis. *Annals of the rheumatic*
481 *diseases* **76**, 914-922 (2017).

482 49 Loi, F. *et al.* Inflammation, fracture and bone repair. *Bone* **86**, 119-130 (2016).

483 50 Liu, J. *et al.* Macrophage polarization in periodontal ligament stem cells enhanced
484 periodontal regeneration. *Stem cell research & therapy* **10**, 1-11 (2019).

485 51 Ma, C., Kuzma, M. L., Bai, X. & Yang, J. Biomaterial-based metabolic regulation in
486 regenerative engineering. *Advanced Science* **6**, 1900819 (2019).

487 52 Saborano, R. *et al.* Metabolic reprogramming of macrophages exposed to silk, poly
488 (lactic-co-glycolic acid), and silica nanoparticles. *Advanced Healthcare Materials* **6**,
489 1601240 (2017).

490 53 Gonçalves, R. & Mosser, D. M. The isolation and characterization of murine
491 macrophages. *Current protocols in immunology* **111**, 14.11. 11-14.11. 16 (2015).

492 54 Feoktistova, M., Geserick, P. & Leverkus, M. Crystal violet assay for determining viability
493 of cultured cells. *Cold Spring Harbor Protocols* **2016**, pdb. prot087379 (2016).

494

495 **Acknowledgements.** Euthanized C57BL/6J mice were a gift from RR Neubig
496 (facilitated by J Leipprandt) and the Campus Animal Resources at Michigan State
497 University (MSU). Funding for this work was provided in part by the James and
498 Kathleen Cornelius Endowment at MSU.

499
500 **Author contributions.** Conceptualization, C.V.M. and C.H.C.; Methodology, C.V.M.,
501 S.B.G., and C.H.C.; Investigation, C.V.M., M.O.B., M.M.K. and M.H.; Writing – Original
502 Draft, C.V.M.; Writing – Review & Editing, C.V.M., M.O.B., M.M.K., M.H., S.B.G. and
503 C.H.C.; Funding Acquisition, C.H.C.; Resources, S.B.G. and C.H.C.; Supervision, S.B.G.
504 and C.H.C.

505
506 **Competing interests.** The authors declare no competing interests.